

Latency effects and periodic structures in light-induced frustrated etching of Fe:doped LiNbO₃

Alexander J. Boyland,^{a)} Sakellaris Mailis, Ian E. Barry, and Robert W. Eason
Optoelectronics Research Centre, University of Southampton, Southampton SO17 1BJ, United Kingdom

Malgosia Kaczmarek
Physics Department, Exeter University, Stocker Road, Exeter EX4 4BL, United Kingdom

(Received 22 June 2000; accepted for publication 6 September 2000)

Single crystals of z-cut 0.05% Fe:doped lithium niobate (Fe:LiNbO₃), have been etched in a mixture of HF and HNO₃ acids, under simultaneous illumination from a ~100 mW 488 nm wavelength Ar ion laser light source, focused to power densities of ~50 W cm⁻² at the crystal surface exposed to the etchant. Etching is partially inhibited in illuminated regions, and the degree of inhibition shows a systematic latency: sites illuminated early in the etch run resist further etching even after the light is removed. Etched structures additionally exhibit regular periodic features of ~0.5 μm scale length. Details of these structures are shown, and the latent etching effect is discussed. © 2000 American Institute of Physics. [S0003-6951(00)00844-5]

Structuring of photonic and optoelectronic materials at sub-μm scale lengths continues to have considerable interest in areas such as photonic crystal solids,¹ Bragg grating fabrication,² tips for scanning probe microscopes, and the developing area of optical MEMS.³ In all cases, such structuring requires methodologies for, and accurate control of, the patterning, processing and subsequent revealing stages for the features to be fabricated. In this letter, we report new results in the microstructuring of iron doped lithium niobate single crystals for which the normal etch characteristics are modified through a photoelectrochemical process at the lithium niobate/etchant interface. We observe a latent effect, in which illumination of the sample has a marked effect on subsequent etching behavior for periods of at least several hours after the illumination has been removed, and show arrays of periodic features of ~0.5 μm scale lengths that result from this latent etch behavior.

Initial results in light induced frustrated etching (LIFE) in Fe:doped LiNbO₃ have already been reported.⁴ These preliminary results however were directed mainly at total suppression of etching, and additionally used more heavily doped (0.2%) Fe:LiNbO₃. Details of the LIFE process can be found in Ref. 4, but for clarity we briefly review the etch frustration procedure, whose implementation is illustrated in Fig. 1.

The etch cell is constructed from stainless steel and PTFE, which has good etch resistance from the 1:2 mixture of HF and HNO₃ acids used. The LiNbO₃ crystal was a z-cut oriented, 0.5 mm thick sample of dimensions 10 mm square, doped with 0.05 wt% Fe, and supplied by Cstech, China, oriented with the -z face uppermost. When exposed to the etchant, the -z face will etch at a rate of ~1 μm per hour at room temperature, while the +z face remains almost totally unaffected. However, when moderate cw visible laser power densities (~1 W cm⁻²) are directed at the LiNbO₃ interface undergoing etching this normal etch rate can be drastically

modified, yielding complete etch frustration at power densities of ~100 W cm⁻², and partial frustration for power levels down to ~1 W cm⁻². The laser light used here, unlike that reported for Ref. 4, was passed through a spatial filter assembly, consisting of two microscope objectives and 25 μm diameter pinhole to ensure clean Gaussian beam illumination.

The explanation for this behavior concerns the photoelectrochemical modification of etching through light-induced charge migration from the Fe ion dopant. There is also the possibility of an electrochemical interaction caused by the contribution made by the bulk photovoltaic effect, which can be large in such relatively heavily doped crystals.⁵ The choice of laser wavelength may also be important and we have investigated cw illumination at 488 nm as well as pulsed illumination using a KrF excimer laser at 248 nm.

Figure 2 illustrates schematically the procedure adopted

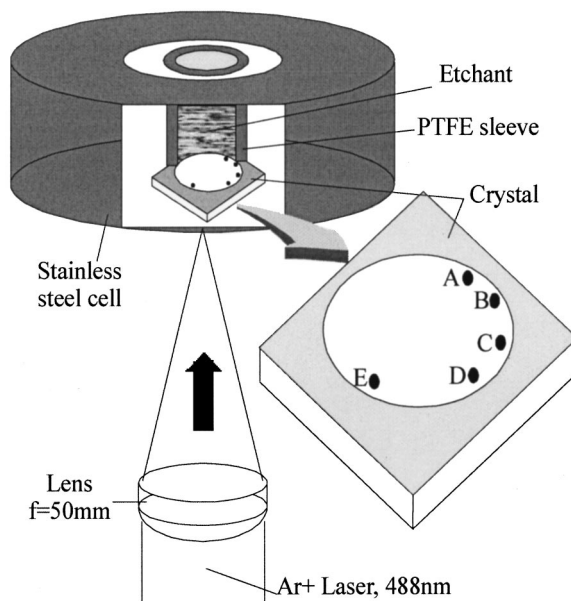


FIG. 1. Schematic arrangement of cell used to conduct LIFE experiments with Fe:doped LiNbO₃.

^{a)}Electronic mail: ajb@orc.soton.ac.uk

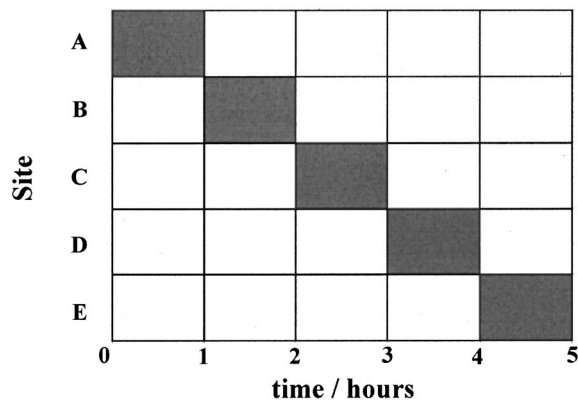


FIG. 2. Schematic to illustrate the temporal sequencing of illumination used at each etch site A–E. The shaded areas represent periods of illuminated etching.

to determine whether any latent effects were present in the LIFE process for illumination with 488 nm light. Five sites (labeled A–E) were exposed to laser illumination, at the same power density, each for a 1 h duration. The total etch run lasted 5 h, and was conducted at room temperature without the cell being disturbed or adjusted, other than to turn it around to expose a new site to laser illumination. Site A therefore had 1 h of illuminated etching, followed by 4 h of unilluminated etching, whereas site E had the complementary procedure of 4 h of unilluminated etching, followed by a final hour of illuminated etching. After 5 h, the cell was dismantled, and the LiNbO₃ sample was examined under optical and scanning electron microscopy (SEM), and alphastep profilometer measurements were made of the respective heights of the material left unetched at each site.

Figure 3 shows the results from the alphastep measure-

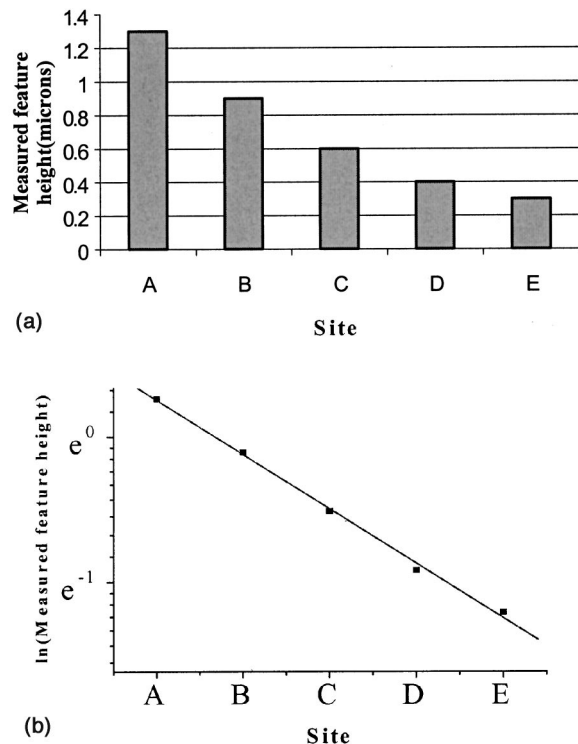


FIG. 3. Histogram of heights of etched material at each site (A–E), presented as a linear plot (a), and a semilogarithmic plot (b).

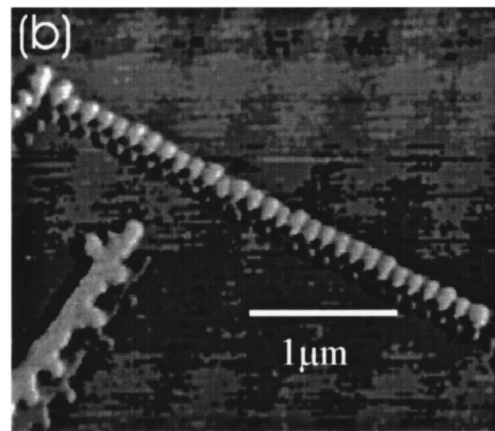
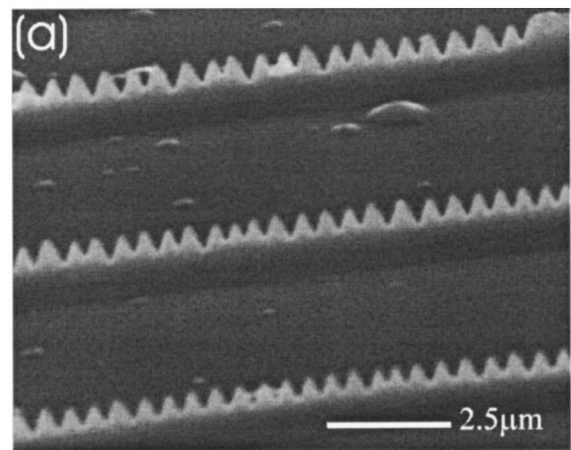


FIG. 4. (a) SEM image for site A which was illuminated by cw. Ar ion light at 488 nm; (b) AFM image for 0.2% doped LiNbO₃ irradiated by excimer laser light at 248 nm.

ments from all five sites. It is clear that there is a systematic trend in the measured heights of material that remains unetched, and that this reflects the illumination sequencing adopted. Figure 3(a) shows the raw data, while Fig. 3(b) has been replotted on a semilogarithmic scale. The linear fit obtained from Fig. 3(b) indicates that a characteristic time constant applies to the process by which the etching can remain partially frustrated, and that this lies in the region of a few hours, at this temperature, and dopant concentration.

Figure 4(a) shows a SEM image of features observed from site A, which was illuminated for the first hour only. What is immediately apparent is the regular spiked features that appear to characterize these LIFE results: The periodicity shown here is very close to 0.5 μm. We have observed very similar results for both 0.05 wt% and 0.2% Fe:doped LiNbO₃ that has been irradiated by excimer laser pulses from a KrF 248 nm source, and subsequently etched. In both these cases, the periodicity was smaller than that reported here, with a value closer to 0.125 μm being observed with the 0.2% doped samples. Increased doping clearly leads to increased mobile charge available, and we regard this correlation as significant in determining the periodicity achievable.

Figure 4(b) shows an AFM scan of an excimer irradiated 0.2% doped sample that has been subsequently etched: the results are quantitatively very similar, showing lines of frustrated etching with discrete spiked features. The exact topography of the spiked tips is not necessarily faithfully repro-

duced via the AFM, but the figure clearly shows the obvious similarities.

Although LiNbO₃ has often been regarded as macroscopically homogeneous, except for slight growth variations parallel to the *c* axis, it has a number of intrinsic defects. For example, LiNbO₃ segregation at the surface⁶ can give rise to micrometer high structures rising above the wafer surface and accompanied by shallow, micrometer deep grooves. These grooves are associated with Nb diffusion that occurs only at the crystal surface and along defect planes. As a result, “rope-like ladders” structure,⁶ extending inside the wafer, can be detected. Moreover, low-angle grain boundaries along the *z* axis, voids, and small decanted interfaces⁷ have also been observed and linked with the crystal growth and pulling rate.

LiNbO₃ is also capable of tolerating high concentrations of impurity ions.⁸ Some of these structural inhomogeneities, such as filaments and defect planes, are linked to diffusion of impurity atoms and vacancies. These inhomogeneities⁹ can strongly influence piezo, pyro, and ferroelectric properties of LiNbO₃. For example, a significant decrease in diffraction efficiency has been observed for gratings with spacings between 0.5 and 1 μm.⁹

One of the characteristic features of LiNbO₃ is its strong photovoltaic effect,¹⁰ the strength of which depends on the level of Fe doping—the major impurity found in LiNbO₃. Its two valence states, Fe²⁺ and Fe³⁺, play a major role: photovoltaic tensor elements depend linearly on the Fe²⁺ concentration, while photoconductivity is determined by electron transfer from Fe²⁺ to Fe³⁺ centers.¹¹ This transfer of charges is particularly pronounced in the visible, near-absorption bands of Fe²⁺ at approximately 2.6 eV (476 nm) and Fe³⁺ at 2.55 (488 nm) and 2.95 eV (420 nm).

Light induced photovoltaic current means that excited electrons move through the crystal along the *c* axis with a preferred direction of motion. It is the inhomogeneities and their local electric fields that determine the charge transfer mechanism.⁹ As has been suggested,⁹ there is no significant light absorption in perfect crystalline regions; absorption takes place only where defect regions exist. These discretely spaced inhomogeneities serve as donors and traps for elec-

trons. Photovoltaic current flowing in one direction and only through defects leads to accumulation of charges and subsequently to repolarization.¹² Repolarization can not only create microdomains, but also cause larger defects developing into wafer fractures. If a wafer is then exposed to etchant, the accumulation of charges affects the diffusion of fluorine ions (from the acid) and hence the difference in etching rates. Etching, therefore, can work as a method of revealing the patterns of inhomogeneities or filaments that contain charges.

Work is currently in progress to further develop this model, and control the periodic structuring at the submicron level using both static and scanned light field distributions. One obvious application area concerns photonic crystal solids, but the MEMS and MOEMS area is also where we see this technique as having immediate relevance.

The authors would like to acknowledge the Engineering and Physical Sciences Research Council (EPSRC) for a post-graduate research award for A.J.B. Thanks also go to Dr. Barbara Cressey, at the Electron Microscopy Center for use of SEM facilities, and to Dr. Karsten Buse for collaboration and ongoing discussions on etching in LiNbO₃.

¹J. D. Joannopoulos, R. D. Meade, and J. N. Winn, *Photonic Crystals* (Princeton University Press, Princeton, NJ, 1995).

²R. Kashyap, *Fibre Bragg Gratings* (Academic, San Diego, CA, 1999).

³S. J. Walker and D. J. Nagel, Naval Research Laboratory Report No. NRL/MR/6336-99-7975 (1999).

⁴I. E. Barry, G. W. Ross, P. G. R. Smith, R. W. Eason, and G. Cook, *Mater. Lett.* **37**, 246 (1998).

⁵J. P. Huignard and P. Gunter, *Photorefractive Materials and Their Applications: Topics in Applied Physics* (Springer, Berlin, 1989), Vol. 61.

⁶E. Born, J. Hornsteiner, T. Metzger, and E. Riha, *Phys. Status Solidi A* **177**, 383 (2000).

⁷T. Suzuki, *J. Mater. Sci.* **30**, 2873 (1995).

⁸O. F. Schirmer, O. Thiemann, and M. Wohlecke, *J. Phys. Chem. Solids* **52**, 185 (1991).

⁹I. F. Kanaev and V. K. Malinovsky, *Ferroelectrics* **218**, 27 (1998).

¹⁰A. M. Glass, D. von der Linde, and T. J. Negran, *Appl. Phys. Lett.* **25**, 233 (1974).

¹¹R. Sommerfeldt, L. Holtmann, E. Kratzig, and B. C. Grabmaier, *Phys. Status Solidi A* **106**, 89 (1988).

¹²H. Nagata, J. Ichikawa, M. Sakima, K. Shima, and F. M. Haga, *J. Mater. Res.* **15**, 17 (2000).